JETIR.ORG ISSN: 2349-5162 | ESTD Year : 2014 | Monthly Issue
JOURNAL OF EMERGING TECHNOLOGIES AND INNOVATIVE RESEARCH (JETIR)
An International Scholarly Open Access, Peer-reviewed, Refereed Journal

Regression model for heat transfer behavior of Casson fluid between two parallel plates.

C. Sulochana[1*], Nityanand[1]

1. Department of mathematics, Gulbarga University, Kalaburagi, Karnataka, India.

Abstract: Non-Newtonian liquids have wide range of applications in many industries such as food processing, coolants in nuclear reactors, polymer extrusions etc. This present communication explores squeezing flow of Casson fluid between two parallel surfaces with partial slip effect. Similarity transformations are applied to convert the fluid flow governing equations into ordinary differential equations and then solved by MATLAB software with the help bvp4c algorithm. Statistical analysis is performed by developing a linear regression model for skin friction coefficient, Nusselt number and Sherwood number to predict heat and mass transfer rates. Casson parameter and magnetic parameter increases skin friction. Higher values of Lewis number show a diminishing concentration profile.

Index Terms - Regression analysis, Casson nanofluid, Squeezing flow, bvp4c method.

I. INTRODUCTION

Over the past decade nanofluids are in demand due to their thermo physical properties with promising results in enhancing heat transfer rate. Many researchers conducted experimental and theoretical investigations to understand the heat transport capacity of different nanomaterials. Sheikholeslami et al.[1] examined two phase simulation of nanofluid flow and heat transfer between parallel surfaces. Nanofluid hydrothermal character in presence of variable magnetic field is studied analytically by Sheikholeslami and Ganji [2]. The unsteady flow of a nanofluid squeezed between two parallel plates is modelled by a coupled system of nonlinear ordinary differential equations and a new approach based on the Chebyshev wavelet expansion is proposed by Gupta and Saha Ray [3].Sheikholeslami et al.[4] reported that the behaviour of continuous nanofluid flow between parallel plates in the presence of a uniform magnetic field is investigated in terms of heat and mass transfer .Mohyud-Din et al.[5] examined a rotating system with nanofluid moving between parallel plates, as well as three-dimensional heat and mass transfer using magnetic phenomena. It has been found that thermophoresis and Brownian motion parameters are directly related to heat transfer but inversely related to concentration profiles. The effect of variable magnetic field on nanofluid flow and heat transfer analysis between two parallel disks is scrutinized by Hatami et al.[6]. In this work noticed that the direct relationship between the Nusselt number, the thermophoretic parameter, and the Brownian motion parameter.

In a rotating system, the impacts of electro-magneto-hydrodynamics on nanofluid flow and heat transfer properties are explored by Rokni et al. [7]. Researchers have studied the magnetic parameter, electric parameter and Reynolds number all increase with an increase in the Nusselt number, whereas the rotation parameter causes a drop in the Nusselt number. For the first time, an investigation done by Rashidi et al.[8] is made into the effects of an effective Prandtl number model on the nano boundary layer, steady, two-dimensional, and laminar flow of an incompressible Al_2O_3 - H_2O and Al_2O_3 - $C_2H_6O_2$ nanofluid over a vertical stretching sheet. A.S.Dogonchi et al.[9] investigated how MHD nanofluid between infinite parallel plates squeezes and transfers heat while also experiencing the thermal radiation effect. In which results indicate that as the radiation parameter increases, the temperature profile and Nusselt number also increases. Magodora et al.[10] numerically solve the equations for the flow of a hydromagnetic nanofluid through semi-infinite parallel plates under the assumption that both thermal radiation and a chemical reactions are important and existent. Saeed Ehsan Awan et al. [11] study presents a novel application of numerical computing paradigm to examine the cumulative effects of both electric and magnetic fields on a micropolar nanofluid confined by two parallel plates in a rotating system. A Poiseuille flow it is a flow between two flat plates is studied numerically by Mostafa Mahdavi et al.[12] to determine the effects of nanoscale particles present in the flow. Numerical analysis on the behaviour of stable Casson nanofluid between parallel plates in the presence of a constant magnetic field done by El Harfouf et al.[13]. The findings of this study can aid engineers in making improvements, and researchers can work on this kind of issue more quickly and simply. Bilal et al. [14] studied and noticed that Ionic fluids have a major advantage over conventional solvents regardless of their difficulties with recycling and a overlook the impacts of the magnetic field, heat generation, chemical reaction, and activation energy are also explored together with the fluid flow phenomenon. In order to assess the effectiveness of heat exchangers in the fluid flow via tandem tubes between two parallel plates, the effect of using nanofluids and flat tubes simultaneously is researched and analysed by Mein Darbari et al.[15].The obtained results demonstrate that heat transfer and pressure loss are simultaneously reduced by modifying the cross-section and further flattening. Yaseen et al.[16] investigated that the symmetry of the hybrid nanofluid ($M_OS_2 - SiO_2 / H_2O - C_2H_6O_2$) and the MHD squeezing nanofluid (MoS_2 / H_2O) flow between the parallel plates, the findings of this work have implications for a number of thermal systems, engineering and industrial processes that use hybrid nanofluids and nanofluids for cooling and heating. M.B.Arain et al.[17] investigated the nanofluid bioconvection flow across a pair of vertical parallel plates in the presence of activation energy. This research shows the physical significance of various changing factors on the profile of motile microbes, temperature distribution, and nanoparticle concentration. In next, Through the use of computational analysis, the properties of a hybrid nanofluid flow containing copper (Cu) and cobalt ferrite ($CoFe_2O_4$) nanoparticles (NPs) across a squeezing plate have been examined by Murtaza et al.[18]. It's observed that when compared to the nanofluid, the hybrid nonliquid is found to have a higher capacity for velocity and energy transmission rate. Arshad et al. [19] examines the two distinct hybrid nanofluid flows between two parallel plates that are positioned at two different heights, y_0 and y_h. In this research water-based hybrid nanofluids are obtained by using Al_2O_3, TiO_2 and Cu as nanoparticles, respectively. Steady electro-magnetohydrodynamic flow of a

micropolar nanofluid in the attendance of reactive Casson fluid passing through parallel plates influenced by the rotating system with the implementation of Buongiorno nanofluid model is examined by Shamshuddin and Ibrahim [20]. Abida Shaheen et al.[21] examined the magnetohydrodynamic hybrid nanofluid flows of copper-oxides and titanium dioxide in water ($CuO + TiO_2$) between two parallel plates utilising walls suction/injection under the influence of a magnetic field and thermal radiation. Between vertical parallel plates, a hybrid nanofluid flow with Gold and Magnesium oxide nanoparticles (Au/MgO-NPs) suspended in it is studied by Bhatti et al.[22]. Umar Farooq et al.[23] reported that the combustion process requires proper cooling systems due to the high combustion temperatures. The majority of chambers in liquid propellant engines employ regenerative cooling. In view of the above cited research works and based on importance of squeezing flows in hydrodynamic machines, lubrication and other industrial application we have carried out a theoretical analysis on squeezing nanofluid flow and such works found in the literature to the best of authors knowledge.

1. Problem Formulation

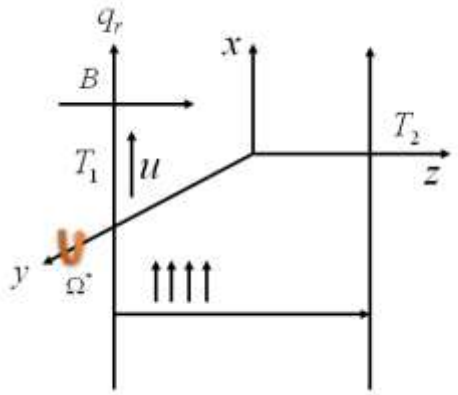

Fig. 1 Geometry of the problem

Consider a vertical channel with parallel plates and a two-dimensional laminar incompressible electrically conducting Casson fluid flow. The x-axis is chosen in vertical direction of the plates and It is assumed that channel is rotating about y axis with a uniform angular velocity Ω .With this assumption the governing equations can be framed as follows:

$$\frac{\partial u}{\partial x}+\frac{\partial u}{\partial y}=0, \tag{1}$$

$$u\frac{\partial u}{\partial x}+v\frac{\partial u}{\partial y}+2\Omega w=v\left(\frac{\beta+1}{\beta}\right)\frac{\partial^2 u}{\partial y^2}-\frac{\sigma B^2\left[u+mw\right]}{\rho\left(1+m^2\right)}+g\beta_T\left[T_1-T_2\right]+g\beta_c\left[C_1-C_2\right], \tag{2}$$

$$u\frac{\partial w}{\partial x}+v\frac{\partial w}{\partial y}-2\Omega w=v\left(\frac{\beta+1}{\beta}\right)\frac{\partial^2 w}{\partial y^2}+\frac{\sigma B^2\left[mu+w\right]}{\rho\left(1+m^2\right)}$$

(3)

$$u\frac{\partial T}{\partial x}+v\frac{\partial T}{\partial y}=\alpha\frac{\partial^2 T}{\partial y^2}+\frac{\mu}{\rho C_P}\left(\frac{\beta+1}{\beta}\right)\left(\frac{\partial u}{\partial y}\right)^2+\frac{\sigma B^2\left[u^2+w^2\right]}{\rho C_p}-\frac{\partial q}{\partial y}+\frac{Q\left(T-T_\infty\right)}{\rho C_P},$$

(4)

$$u\frac{\partial C}{\partial x}+v\frac{\partial C}{\partial y}=D_m\frac{\partial^2 C}{\partial y^2}-K_0\left[C-C_\infty\right], \tag{5}$$

The boundary conditions are:

$$\left.\begin{aligned} &u=cx,\ v=0,\ w=o,\ T=T_1,\ C=C_1,\ y=-a\\ &u=0,\ v=0,\ w=0,\ T=T_2,\ C=C_2,\ y=+a\end{aligned}\right\} \tag{6}$$

The radiative heat flux in eq. (4) can be solved by applying Roseland approximation defined as,

$$q=-\frac{4\sigma^c}{3k^c}\frac{\partial T'^4}{\partial y'} \tag{7}$$

Expansion of T^4 in a Taylor series about T_0 and neglecting the higher order terms gives

$$T'^4\cong 4T_0^3T-3T_0^3 \tag{8}$$

From Eq. (8), equ. (4) becomes,

$$u\frac{\partial T}{\partial x}+v\frac{\partial T}{\partial y}=\alpha\frac{\partial^2 T}{\partial y^2}+\frac{\mu}{\rho C_p}\left(1+\frac{1}{\beta}\right)\left(\frac{\partial u}{\partial y}\right)^2+\frac{\sigma B^2}{\rho C_p}\left(u^2+w^2\right)+\frac{16\sigma^c T^3}{3k^c}\frac{\partial^2 T}{\partial y^2} \tag{9}$$

Applying the similarity transformation,

$$\eta=y\sqrt{\frac{c}{v}},\ u=cxf'(\eta),\ w=cxg(\eta),\ \theta(\eta)=\frac{T-T_2}{T_1-T_2},\ C(\eta)=\frac{C-C_2}{C_1-C_2}, \tag{10}$$

the equations (2), (3), (5) and (9) reduces to,

$$\left(\frac{\beta+1}{\beta}\right)f'''+ff''-f'^2-2R^2g-\frac{H^2}{\left(1+m^2\right)}\left(f'+mg\right)+Gr\theta+Gc\phi=0, \tag{11}$$

$$\left(\frac{\beta+1}{\beta}\right)g'''+fg'-gf'+2R^2f'+\frac{H^2}{\left(1+m^2\right)}\left(f'+mg\right)=0, \tag{12}$$

$$\left(1+\frac{4Nr}{3}\right)\theta''+\Pr f\theta'+Br\left(1+\frac{1}{\beta}\right)f''^2+Br\frac{H^2}{\left(1+m^2\right)}\left(f'^2+g^2\right)^2+Q_0\theta=0, \tag{13}$$

$$\phi''+Scf\phi'-\gamma Sc\phi=0, \tag{14}$$

and boundary conditions in dimensionless form can be written as,

$$\left.\begin{aligned} &f(-1)=0,\ f'(-1)=0,\ g(-1)=0,\ \theta(-1)=1,\ \phi(-1)=1,\\ &f'(1)=0,\ g(1)=0,\ \theta(1)=0,\ \phi(1)=0\end{aligned}\right\} \tag{15}$$

Where,

$$H^2=\frac{\sigma B_0{}^2}{\rho C},\ R=\frac{\Omega^*}{C},\ Gr=\frac{g^*\beta^*\left(T_1-T_2\right)}{C^2x},\ Br=\frac{\mu C^2x^2}{k\left(T_1-T_2\right)},\ Ra=\frac{4\sigma^cT^3{}_\infty}{k^ck}$$

$$\alpha=\frac{k}{\rho C_P},\ Gc=\frac{g^*\beta^c\left(C_1-C_2\right)}{C^2x},\ \nu=\frac{\mu}{\rho},\ Sc=\frac{\upsilon}{\alpha},\ \Pr=\frac{\upsilon}{\alpha},$$

$$k_f=\frac{k^*}{c},\ \lambda_1=\frac{DT_0{}^2\left(C_1-C_2\right)^2}{k\left(T_1-T_2\right)},\ \lambda_2=\frac{DT_0\left(C_1-C_2\right)}{k\left(T_1-T_2\right)},\ \Omega=\frac{T_1-T_2}{T_0}. \qquad (16)$$

The following are physical quantities of interest in dimensionless form, the primary and secondary skin friction coefficients (It determines the rate of shear stress at the plate due to primary and secondary flow), the Nusselt number (measuring heat transfer rate) and local Sherwood number (which measures the rate of mass transfer).

$$\left(\mathrm{Re}_x\right)^{\frac{1}{2}}C_f=-\left(1+\frac{1}{\beta}\right)f''(-1),\left(\mathrm{Re}_x\right)^{\frac{1}{2}}C_f=-\left(1+\frac{1}{\beta}\right)g'(-1),$$

$$Nu\left(\mathrm{Re}_x\right)^{\frac{-1}{2}}=-\theta'(-1),\ Sh\left(\mathrm{Re}_x\right)^{\frac{-1}{2}}=-\phi^1(-1) \qquad (17)$$

2. Numerical procedure

We have used MATLAB software built in function bvp4c to resolve equations (11)-(14) with boundary conditions (15).

As a prerequisite for writing code, let us consider the following assumptions.

$$f=F_1,\ f^1=F_2,\ f''=F_3,g=F_4,g^1=F_5,g''=F_6,\theta=F_7,\theta'=F_8,\phi=F_9,\phi^1=F_{10}.$$

Next, by using equations (11)-(14) with boundary conditions (15).

We can obtain a following system of ODEs of first order:

$$
\begin{aligned}
F_1' &= f_2,\\
F_2' &= f_3,\\
F_3' &= \left(\frac{\beta}{\beta+1}\right)\left[-f_1 f_3 + f_2^{\,2} + 2R^2 f_4 + \frac{H^2}{\left(1+m^2\right)}\left(f_2 + m f_4 - Grf_7 - Gcf_9\right)\right],\\
F_4' &= f_5,\\
F_5' &= f_6,\\
F_6' &= \left(\frac{\beta}{\beta+1}\right)\left[-f_1 f_5 + f_4 f_2 - 2R^2 f_2 - \frac{H^2}{\left(1+m^2\right)}\left(f_2 + m f_4\right)\right],\\
F_7' &= f_8,\\
F_8' &= \left(\frac{3}{3+4Nr}\right)\left[-\Pr\, f_1 f_8 - Br\left(1+\frac{1}{\beta}\right) f_3^{\,2} - B_r \frac{H^2}{\left(1+m^2\right)}\left(f_2^{\,2} + f_4^{\,2}\right)^2 - Q_0 f_7\right],\\
F_9' &= f_{10},\\
F_{10}' &= -Scf_1 f_{10} + \gamma Scf_9.
\end{aligned}
\tag{18}
$$

With boundary conditions

$$
\begin{aligned}
&Fa(1)=0, Fa(2)=0, Fa(4)=0, Fa(7)=1, Fa(9)=1,\\
&Fb(2)=0, Fb(4)=0, Fb(7)=0, Fb(9)=0.
\end{aligned}
\tag{19}
$$

After converting the aforementioned system to MATLAB code, we can run it to obtain the desired results in the form of graphs.

3. Result and Discussion

To investigate various flow scenarios, boundary conditions and the numerical solution of the dimensionless equations (11–14) are used. the formulation for fluid entropy generation is modified because of reflect the result. In figures and tables, the effects of the Hartman number (H^2), the Casson fluid parameter (β), the Hall parameter (m), the radiation parameter (Ra), the Schmidt number (Sc), and the chemical reaction parameter (k_f) on fluid velocity, fluid temperature, and other physical parameters are shown. For the aforementioned parameters, the following values are typically used: H =1.5, m =0.5, Pr =0.71, Br =0.5, Ω =1, Sc=0.1, k_f =0.2, β =1, R =1, Ra =0.1, Gr =1, Gc =1, λ_1=0.1, λ_2 =0.1.

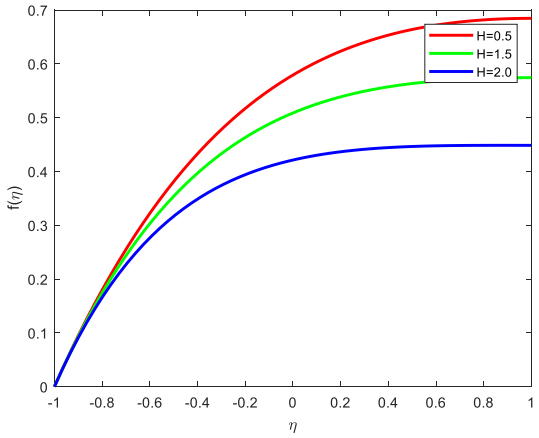

Fig. 2a. Primary velocity profile for Hartmann number

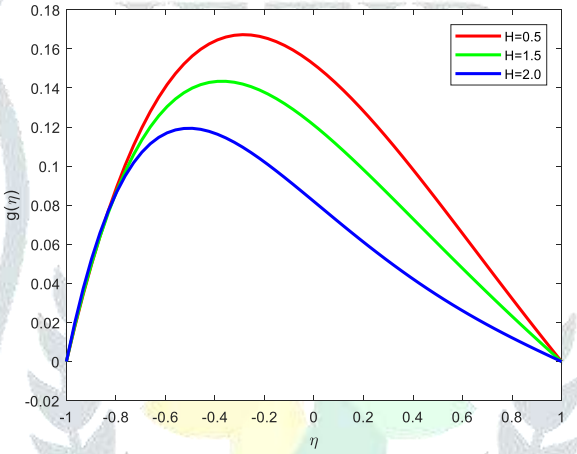

Fig. 2b. Secondary velocity profile for Hartmann number

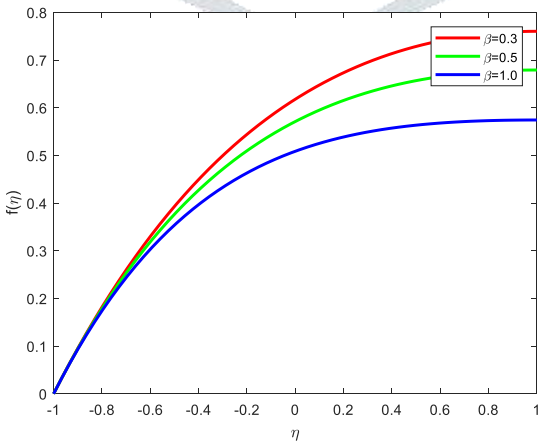

Fig. 2c. Primary velocity for Casson nanofluid parameter

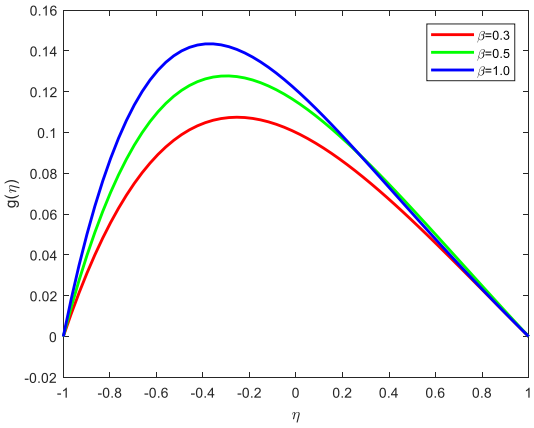

Fig. 2d Secondary velocity profile for Casson nanofluid parameter

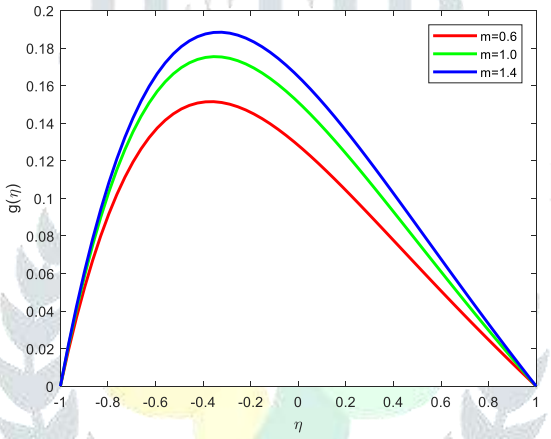

Fig. 2e: Primary velocity profile for Hall Current Parameter.

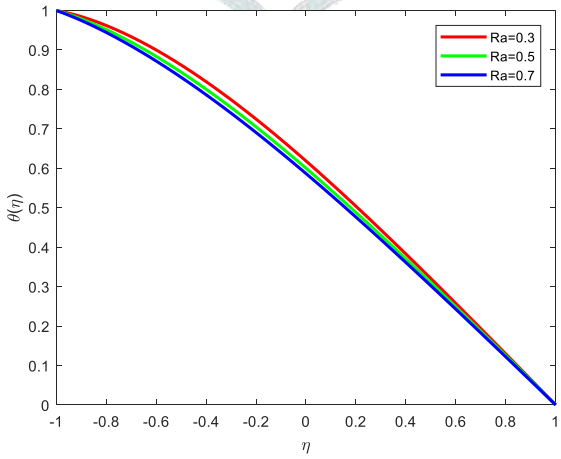

Fig. 2f: Secondary velocity profile for Hall Current Parameter.

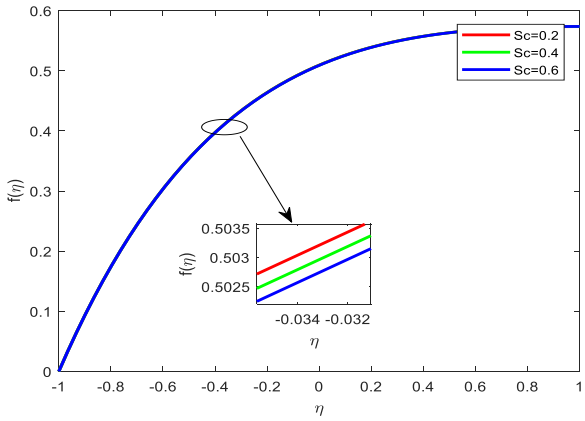

Fig. 2g: Primary velocity profile for Schmidt number.

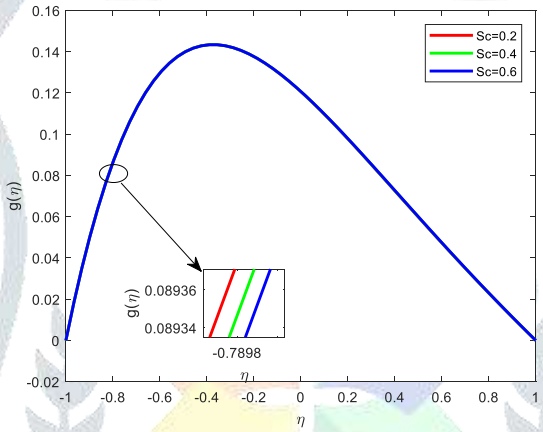

Fig. 2h: Secondary velocity profile for Schmidt number.

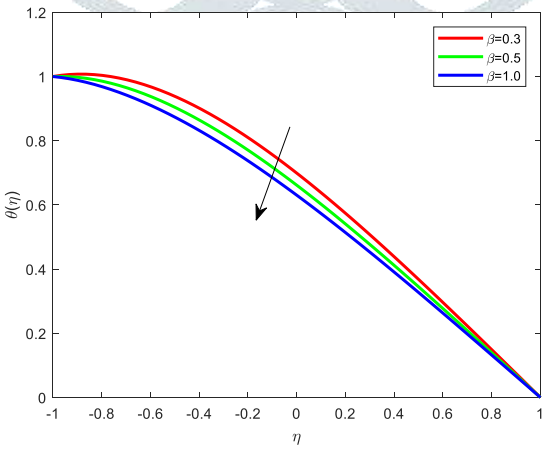

Fig. 3a. Temperature profile for Casson parameter.

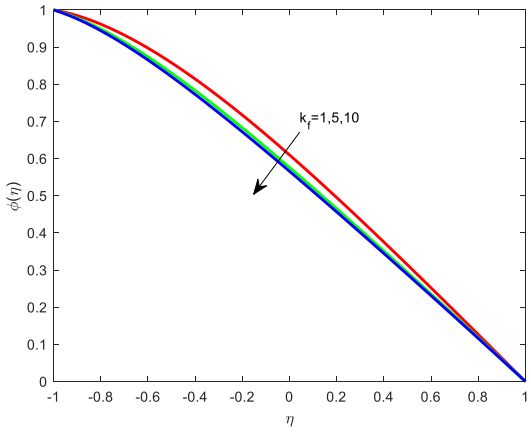

Fig. 3b. Temperature Profile for Radiation parameter.

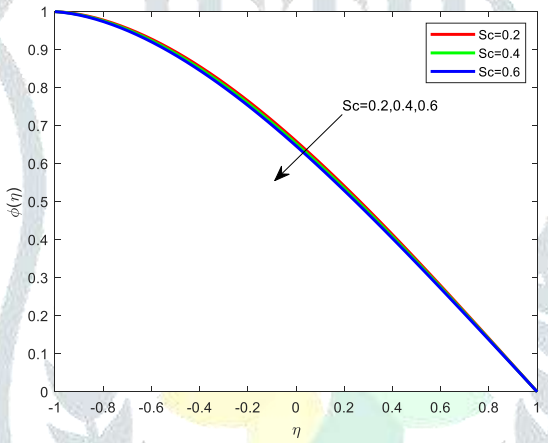

Fig. 4a: Concentration profile for chemical reaction parameter.

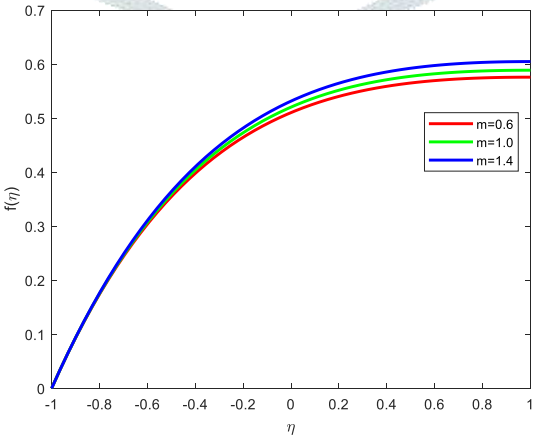

Fig. 4b: Concentration profile for Schmidt number.

Table-1: Computation of skin friction coefficient, Nusselt number and Sherwood number for various physical parameters.

	Gr	Gc	β	Skin friction coefficient	Nusselt number	Sherwood number
0.5				2.1314	0.5413	0.0995
1				2.7908	0.56344	0.0269
1.5				3.8016	0.6226	0.0056
	0.1			2.7480	-0.5744	0.0290
	0.2			2.7694	-0.5689	0.0279
	0.3			2.7908	-0.5634	0.0269
		0.1		2.7487	-0.5693	0.0277
		0.2		2.7908	-0.5634	0.0269
		0.3		2.8328	-0.5575	0.0259
			0.1	4.1727	-0.3384	-0.1340
			0.3	3.4246	-0.4384	-0.0299
			1	2.7955	-0.5632	0.0728

The effects of the Hartmann number, Casson fluid parameter, Hall current parameter, and Schmidt number on fluid velocity are shown in above Figures 2a–h. A rise in the values of the Hartman number, Casson fluid parameter, and Schmidt number retards fluid velocity. On the other side, as the Hall parameter rises, the velocity increases.

It is evident that Fig. 2a,2b are illustrates the effect of the Hartman number on fluid velocity. As Hartman number values change, fluid velocity and boundary layer thickness slow down. This observed phenomenon takes place when the imposed magnetic field induces current in the electrically conducting fluid, resulting in a resistive-type force that reduces fluid velocity. As seen in Fig. 2c, a rise in the Casson parameter (β) corresponding to a decrease in the yield stress, increases fluid viscosity, which results in a decrease in fluid velocity and boundary layer thickness at the top part of the channel. According to Fig. 2e and f, fluid velocity is induced as the value of the Hall current parameter (m) rises. This is due to more resistance to the damping effect of the applied magnetic field at higher values of the Hall parameter, which causes an increase in fluid velocity. According to Fig. 2g and h, a rise in the Schmidt number causes a slowing in fluid velocity because it increases the effective diffusivity of the medium. Schmidt number is the ratio of momentum diffusivity to mass diffusivity.

Figure 3a and 3b show how the Hartmann number, Hall current parameter, and thermal radiation parameter affect fluid temperature. As the Casson fluid parameter (β) is increased in Fig. 3a, the fluid temperature and thermal boundary layer also rise. This occurs as a result of the fluid's lower effective viscosity. The increase in the Rosseland means absorption coefficient term (K^C), which shows as a denominator in the term that represents thermal radiation $\left(Ra = 4\sigma^c T_0'^3 / kk^c\right)$ in Fig. 3b, causes the fluid temperature to rise. The impact of the Schmidt parameter and is shown in Fig. 4a, b. It has been seen that the concentration profile declines as the parameter values rise. As the Schmidt number increases, a decrease in fluid concentration is attributed to an increase in mass diffusion rate.

A common framework for determining relationships between linear independent variables is regression analysis. With so many dependent variables in the heat transfer phenomenon, estimating the rise of heat transfer can be fairly difficult. In order to match the data and reliably forecast the output, a model is

needed. We focused on creating regression models for the Nusselt numbers of various nanoparticle volume fractions in order to determine the better heat transmission rate.

Regression equations for skin friction, Nusselt number and Sherwood number are as follows:

Skin friction coefficient $C_f = 2.8607 + 0.6029H - 1.0714Gr - 0.8604Gc - 0.0677\beta$

Nusselt number $Nu_x = -0.3329 + 1.0107H - 1.9545Gr - 1.9200Gc - 0.3895\beta + 0.1434R$

Sherwood number $Sh_x = -0.0413 + 0.01267H + 0.1528Gr + 0.1469Gc + 0.0677\beta$

Finally, Table 1. shows that computation values of skin fraction coefficient, Nusselt number and Sherwood number for various physical parameters. When rising the Hartmann number, it is enhanced the skin friction coefficient and noticed that when accelerate the values of Local Grashof number due to temperature differences and Casson parameter decelerates the Nusselt number. A slight raise in the value of Local Grashof number due to concentration differences that leads to a slight decelerate in the Sherwood number.

4. Conclusion

A study of MHD mixed convection fluid flowing via parallel vertical plates has been considered. Numerous flow characteristics, including the Schmidt number, Casson fluid parameter, Hall parameter, radiation parameter, and chemical reaction parameter, are studied for their effects. This research study is useful in the investigation of blood flow by taking the effects of magnetic fields and yield value into account. Additionally, it is helpful in the control of cancer growth where it aims to overheat the cancerous tissues much above the crucial therapeutic values 42^0 c. Geophysicists could also get knowledge from this inquiry about the interaction between the geomagnetic field and the fluid in the geothermal zone. The followings main outcomes drawn as,

1. Primary fluid velocity is decreased by the Casson parameter, whereas secondary fluid velocity is decreased by the Schmidt number, chemical reaction parameter, and Casson parameter. A rise in the values of the Hall parameter, however, boosts fluid velocity.
2. The temperature of the fluid is decreased by Hall current and radiation parameters, but it is increased by Hartmann number.
3. Bejan number increases when Schmidt number and chemical reaction parameter take the greater values.
4. Casson parameter and Hartmann number impacts reduces the skin friction values.
5. The Casson parameter increases local Nusselt number at the lower plate but decreases it at the upper plate; nevertheless, as the Hartmann number is changed whereas the opposite result is when observed.
6. The local Sherwood number rises at the lower plate but falls at the top plate as both the Schmidt number and the chemical reaction parameter are risen.

Abbreviation

u, v, w	Velocity components
g^*	Acceleration due to gravity
K	Thermal conductivity
Pr	Prandtl number

B	Magnetic parameter
H^2	Hartmann number
T_1, T_2	Fluid temperatures at left and right places respectively
C_1, C_2	Fluid concentrations at left and right places respectively
N_S	Dimensionless entropy generation
Ra	Thermal radiation parameter
R^2	Rotation parameter
Br	Brinkman number
Gr	Local Grashof number due to temperature difference
Gc	Local Grashof number due to concentration differences
Sc	Schmidt number
m	Hall current Parameter
C_p	Specific heat at constant pressure
k_f	Chemical reaction parameter
q_r	Radiative heat flux
D	Mass diffusivity
T	Fluid temperature
C	Concentration
k^c	Rosseland mean absorption coefficient

Greek symbols

β	Casson parameter
β^*	Coefficient of thermal expansion
β^c	Coefficient of expansion with concentration
μ	Dynamic viscosity
υ	Kinematic viscosity
σ	Electrical conductivity
θ	Dimensionless temperature
ϕ	Dimensionless concentration
ψ	Stream function
η	Similarity variable
ρ	Fluid density
α	Thermal diffusivity
Ω	Dimensionless temperature difference
Ω^*	Angular velocity

σ^c Stefan-Boltzman constant

5. ACKNOWLEDGMNENT

The authors express their gratitude to the anonymous reviewers for their insightful recommendations and insightful remarks, which helped to significantly enhance the article.

References

[1] M. Sheikholeslami, M. Hatami, and G. Domairry, "Numerical simulation of two phase unsteady nanofluid flow and heat transfer between parallel plates in presence of time dependent magnetic field," *J. Taiwan Inst. Chem. Eng.*, vol. 46, pp. 43–50, Jan. 2015, doi: 10.1016/j.jtice.2014.09.025.

[2] M. Sheikholeslami and D. D. Ganji, "Nanofluid flow and heat transfer between parallel plates considering Brownian motion using DTM," *Comput. Methods Appl. Mech. Eng.*, vol. 283, pp. 651–663, Jan. 2015, doi: 10.1016/j.cma.2014.09.038.

[3] A. K. Gupta and S. Saha Ray, "Numerical treatment for investigation of squeezing unsteady nanofluid flow between two parallel plates," *Powder Technol.*, vol. 279, pp. 282–289, Jul. 2015, doi: 10.1016/j.powtec.2015.04.018.

[4] M. Sheikholeslami, M. M. Rashidi, D. M. Al Saad, F. Firouzi, H. B. Rokni, and G. Domairry, "Steady nanofluid flow between parallel plates considering thermophoresis and Brownian effects," *J. King Saud Univ. - Sci.*, vol. 28, no. 4, pp. 380–389, Oct. 2016, doi: 10.1016/j.jksus.2015.06.003.

[5] S. T. Mohyud-Din, Z. A. Zaidi, U. Khan, and N. Ahmed, "On heat and mass transfer analysis for the flow of a nanofluid between rotating parallel plates," *Aerosp. Sci. Technol.*, vol. 46, pp. 514–522, Oct. 2015, doi: 10.1016/j.ast.2015.07.020.

[6] M. Hatami, D. Jing, D. Song, M. Sheikholeslami, and D. D. Ganji, "Heat transfer and flow analysis of nanofluid flow between parallel plates in presence of variable magnetic field using HPM," *J. Magn. Magn. Mater.*, vol. 396, pp. 275–282, Dec. 2015, doi: 10.1016/j.jmmm.2015.08.043.

[7] H. B. Rokni, D. M. Alsaad, and P. Valipour, "Electrohydrodynamic nanofluid flow and heat transfer between two plates," *J. Mol. Liq.*, vol. 216, pp. 583–589, Apr. 2016, doi: 10.1016/j.molliq.2016.01.073.

[8] M. M. Rashidi, N. Vishnu Ganesh, A. K. Abdul Hakeem, B. Ganga, and G. Lorenzini, "Influences of an effective Prandtl number model on nano boundary layer flow of γ Al2O3–H2O and γ Al2O3–C2H6O2 over a vertical stretching sheet," *Int. J. Heat Mass Transf.*, vol. 98, pp. 616–623, Jul. 2016, doi: 10.1016/j.ijheatmasstransfer.2016.03.006.

[9] A. S. Dogonchi, K. Divsalar, and D. D. Ganji, "Flow and heat transfer of MHD nanofluid between parallel plates in the presence of thermal radiation," *Comput. Methods Appl. Mech. Eng.*, vol. 310, pp. 58–76, Oct. 2016, doi: 10.1016/j.cma.2016.07.003.

[10] M. Magodora, H. Mondal, and P. Sibanda, "Effect of Cattaneo-Christov Heat Flux on Radiative Hydromagnetic Nanofluid Flow between Parallel Plates using Spectral Quasilinearization Method," *J. Appl. Comput. Mech.*, vol. 8, no. 3, pp. 865–875, Jul. 2022, doi: 10.22055/jacm.2020.33298.2195.

[11] "Numerical Computing Paradigm for Investigation of Micropolar Nanofluid Flow Between Parallel Plates System with Impact of Electrical MHD and Hall Current \textbar SpringerLink." Accessed: May 24, 2023. [Online]. Available: https://link.springer.com/article/10.1007/s13369-020-04736-8

[12] M. Mahdavi, M. Sharifpur, M. H. Ahmadi, and J. P. Meyer, "Nanofluid flow and shear layers between two parallel plates: a simulation approach," *Eng. Appl. Comput. Fluid Mech.*, vol. 14, no. 1, pp. 1536–1545, Jan. 2020, doi: 10.1080/19942060.2020.1844806.

[13] A. El Harfouf, S. Hayani Mounir, and A. Wakif, "Steady Magnetohydrodynamic Casson Nanofluid Flow Between Two Infinit Parallel Plates Using Akbari Ganji's Method (AGM)," *J. Nanofluids*, vol. 12, no. 3, pp. 633–642, Apr. 2023, doi: 10.1166/jon.2023.1947.

[14] M. Bilal *et al.*, "Numerical Analysis of an Unsteady, Electroviscous, Ternary Hybrid Nanofluid Flow with Chemical Reaction and Activation Energy across Parallel Plates," *Micromachines*, vol. 13, no. 6, p. 874, Jun. 2022, doi: 10.3390/mi13060874.

[15] A. Moein Darbari, M. A. Alavi, S. R. Saleh, and V. Nejati, "Sensitivity analysis of nanofluid flow over different flat tubes confined between two parallel plates using Taguchi method and statistical analysis of variance," *Int. J. Therm. Sci.*, vol. 173, p. 107428, Mar. 2022, doi: 10.1016/j.ijthermalsci.2021.107428.

[16] M. Yaseen, S. K. Rawat, A. Shafiq, M. Kumar, and K. Nonlaopon, "Analysis of Heat Transfer of Mono and Hybrid Nanofluid Flow between Two Parallel Plates in a Darcy Porous Medium with Thermal Radiation and Heat Generation/Absorption," *Symmetry*, vol. 14, no. 9, p. 1943, Sep. 2022, doi: 10.3390/sym14091943.

[17] M. B. Arain, A. Zeeshan, M. Sh. Alhodaly, L. Fasheng, and M. M. Bhatti, "Bioconvection nanofluid flow through vertical rigid parallel plates with the application of Arrhenius kinetics: a numerical study," *Waves Random Complex Media*, vol. 0, no. 0, pp. 1–18, Sep. 2022, doi: 10.1080/17455030.2022.2123115.

[18] S. Murtaza, P. Kumam, Z. Ahmad, M. Ramzan, I. Ali, and A. Saeed, "Computational Simulation of Unsteady Squeezing Hybrid Nanofluid Flow Through a Horizontal Channel Comprised of Metallic Nanoparticles," *J. Nanofluids*, vol. 12, no. 5, pp. 1327–1334, Jun. 2023, doi: 10.1166/jon.2023.2020.

[19] M. Arshad *et al.*, "Rotating Hybrid Nanofluid Flow with Chemical Reaction and Thermal Radiation between Parallel Plates," *Nanomaterials*, vol. 12, no. 23, p. 4177, Jan. 2022, doi: 10.3390/nano12234177.

[20] MD. Shamshuddin and W. Ibrahim, "Finite element numerical technique for magneto-micropolar nanofluid flow filled with chemically reactive casson fluid between parallel plates subjected to rotatory system with electrical and Hall currents," *Int. J. Model. Simul.*, vol. 42, no. 6, pp. 985–1004, Nov. 2022, doi: 10.1080/02286203.2021.2012634.

[21] "Thermal transport analysis of squeezing hybrid nanofluid flow between two parallel plates - Abida Shaheen, Muhammad Imran, Hassan Waqas, Mohsan Raza, Saima Rashid, 2023." Accessed: May 24, 2023. [Online]. Available: https://journals.sagepub.com/doi/full/10.1177/16878132221147453

[22] M. M. Bhatti, O. Anwar Bég, R. Ellahi, M. H. Doranehgard, and F. Rabiei, "Electro-magnetohydrodynamics hybrid nanofluid flow with gold and magnesium oxide nanoparticles through vertical parallel plates," *J. Magn. Magn. Mater.*, vol. 564, p. 170136, Dec. 2022, doi: 10.1016/j.jmmm.2022.170136.

[23] U. Farooq *et al.*, "Numerical framework of hybrid nanofluid over two horizontal parallel plates with non-linear thermal radiation," *Int. J. Thermofluids*, vol. 18, p. 100346, May 2023, doi: 10.1016/j.ijft.2023.100346.